

Cellular Detection of Glutathione Using Synthesized Stable Sea Urchin-Like Gold Nanoparticles

Ting Lei Zhao¹, Zhe Zhang², Dan Li¹, Yanxialei Jiang^{1,*}

¹College of Chemistry and Chemical Engineering, Linyi University, Linyi, China

²College of Chemistry and Chemical Engineering, Jinan University, Jinan, China

Email address:

jyxialei@163.com (Yanxialei Jiang)

*Corresponding author

To cite this article:

Ting Lei Zhao, Zhe Zhang, Dan Li, Yanxialei Jiang. Cellular Detection of Glutathione Using Synthesized Stable Sea Urchin-Like Gold Nanoparticles. *International Journal of Biomedical Science and Engineering*. Vol. 10, No. 2, 2022, pp. 54-60.

doi: 10.11648/j.ijbse.20221002.14

Received: May 31, 2022; Accepted: June 15, 2022; Published: June 27, 2022

Abstract: Gold nanoparticles (AuNPs) have been widely studied in a great mass of cellular biomarkers detection and diagnostics due to their unique combination of physical and optical properties. Sea urchin-like gold nanoparticles (SUL-AuNPs) are well characterized multi-thorn gold nanostructures which possess at least four gold nanothorns on spherical gold surface, mimicking the morphology of sea urchin. Compared to spherical AuNPs, SUL-AuNPs showed a wide variety of light absorption and scattering properties, and the Surface-enhanced Raman Scattering (SERS) properties of SUL-AuNPs were also widely studied dependent on their surface morphology. Herein, three different diameters of SUL-AuNPs based on spherical AuNPs seed-mediated growth method by altering the amount of AuNPs in reaction system had been synthesized. The UV-vis spectrum of synthesized SUL-AuNPs displayed a shift from 550 nm to 650 nm compared to spherical AuNPs. FRET method was applied for the detection of GSH in hepatocytes and cell extracts using rhodamine B (RB) functionalized SUL-AuNPs, among the synthesized three different diameters SUL-AuNPs, 100nm RB-SUL-AuNPs displayed highest sensitivity for GSH detection. What's more, all synthesized SUL-AuNPs turned out to be membrane-permeable, and displayed ignorable cytotoxicity, which make SUL-AuNPs promising cellular thiols detection probes. In particular, it should be noted that the application of RB functionalized SUL-AuNPs exemplify ongoing efforts in design and utility of multifunctional nanoplateforms of SUL-AuNPs.

Keywords: FRET, Glutathione, Sea Urchin-Like Gold Nanoparticle, Thiol Detection

1. Introduction

Gold nanoparticles (AuNPs), due to their unique combination of physical and optical properties, have been widely used in a great mass of cellular biomarkers detection and diagnostics [1]. The aggregation of AuNPs resulted in color changes and accelerated the development of a series of assays for cellular biomarkers detections [2-4]. Sea urchin-like gold nanoparticles (SUL-AuNPs) are a newly developed type of multi-thorn gold nanostructures which possess at least four gold nanothorns on spherical gold surface. SUL-AuNPs mimic the shape of sea urchin and the unique structure of SUL-AuNPs showed a wide variety of light absorption and scattering properties. Through altering the initiated amount of spherical gold seeds, hydroquinone, HAuCl₄ in the reaction system, the

size of the synthesized SUL-AuNPs altered and their UV-vis spectrum shifted [5]. The widely studied Surface-enhanced Raman Scattering (SERS) properties of SUL-AuNPs are mostly dependent on their surface morphology and SUL-AuNPs with smaller diameters and longer thorns gave rise to a stronger SERS enhancement [6-9].

Great progression has been made for cellular thiols detection by luminescent or colorimetric sensors [10-13]. Glutathione (GSH), which is well known as the most abundant intracellular thiol [14, 15], plays an influential role in cellular antioxidant defence system [16-19]. Intracellular GSH levels are dramatically affected by oxidative stress, wherefore intracellular detection of GSH is one of the priority among priorities for cellular study [15]. Hence, GSH was selected here as a cellular thiol model for SUL-AuNPs. Fluorescence resonance energy transfer (FRET), which is typically used to measure the

interaction between two molecules labeled with two different fluorophores, the donor and the acceptor, by the transfer of energy from the excited donor to the acceptor [20-23], was selectively utilized for estimating cellular GSH levels [24-26].

Here we synthesized three different sizes of SUL-AuNPs, modified them with rhodamine B (RB) using electrostatic interaction, named as RB-functionalized SUL-AuNPs (RB-SUL-AuNPs), subsequently, as “ON” state of FRET [24].

While in the presence of GSH, GSH competitively react with SUL-AuNPs based on Au-S covalent binding, resulting in the release of RB from SUL-AuNPs, as “OFF” state of FRET, which was used for cellular GSH monitor (Figure 1). Furthermore, the results showed that synthesized SUL-AuNPs are membrane-permeable, and displayed ignorable cytotoxicity, and 100 nm diameter SUL-AuNPs displayed a promising cellular thiols detection properties.

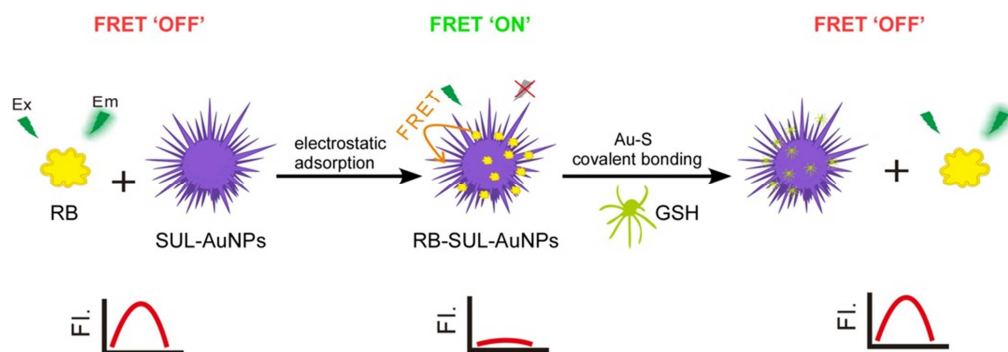


Figure 1. Illustration of GSH detection using RB-SUL-AuNPs coupled with FRET.

2. Material and Methods

2.1. Synthesis of Gold Seeds

The synthesis method of spherical Au seeds was based on the citrate reduction method [27]. Prepare 300 mM HAuCl₄ solution by dissolving 1 g of HAuCl₄·H₂O into 8.09 mL of deionized H₂O. Add 25 μ L 300 mM HAuCl₄ solution and 30 mL of deionized H₂O into a flask and heated to boil. Add 900 μ L of 1 w/v% sodium citrate solution to the boiling solution and kept the mixture in boiling condition until the mixture solution became red. Stir the mixture solution until it cool to room temperature. The Au seeds precipitated out and should be used within one day [28].

2.2. Synthesis of SUL-AuNPs

Dilute 8 μ L of 300 mM HAuCl₄ solution with 9.6 mL of deionized H₂O under vigorous stirring. Subsequently, 100/300/600 μ L of synthesized Au seeds, 22 μ L of 1 w/v% sodium citrate solution, 1 mL of 30 mM freshly prepared hydroquinone solution was added to the diluted HAuCl₄ solution in the order. The mixed solution was kept stirring at room temperature for 30 mins to synthesize different size of SUL-AuNPs [28].

2.3. Preparation of RB-SUL-AuNPs

1 mL of 8.0 μ M RB solution was added to synthesized 3 mL of 8.0 nM SUL-AuNPs solution and interact with each other in dark for 1 hr at room temperature. Subsequently, RB-SUL-AuNPs were precipitated by centrifugation at 8000 rpm for 10 mins. 2 mL deionized H₂O was added and sonicated for 2 mins to obtain RB-SUL-AuNPs solution.

2.4. Detection of GSH

The characterization of RB-SUL-AuNPs by adding

displayed concentrations of GSH solutions was observed at room temperature using UV-vis spectrophotometer. Briefly, 3 mL of RB-SUL-AuNPs solution was added to a series of GSH solutions each with final GSH concentrations ranging from 2 μ M to 1000 μ M. The supernate of the reaction mixture was taken for fluorescence measurement after 1h shaking in dark room for reaction.

2.5. Cell Culture and Flow Cytometry

HepG2 cells and L02 cells used in this study were cultured in DMEM supplemented with 10% fetal bovine serum, 2 mM glutamine, 100 units/mL penicillin/streptomycin, and incubated at 37°C in a humidified atmosphere with 5% CO₂ and 95% air. Intracellular fluorescence express was detected by flow cytometry using cell lysate extract from HepG2 cells and L02 cells. Flow cytometry assay was performed by CytoFLEX flow cytometer (Beckman) with a laser excitation wavelength of 488 nm.

2.6. Assessment of Cell Viability

Cell viability was assessed with CCK-8. Briefly, HepG2 cells and L02 cells incubated with different sizes of SUL-AuNPs for 24 hrs at different concentrations. CCK-8 solution was then added to the cell culture media and incubated for additional 1hr, which were assessed by measuring 450 nm absorbance measurement.

3. Results and Discussion

To synthesis of SUL-AuNPs, spherical AuNPs with a diameter of 20 nm were firstly prepared based on the citrate reduction approach [27]. In this step, citrate acted as the ligand, while both citrate and hydroquinone acted as reductants. As indicated in Figure 2A, a clearly size increase of synthesized SUL-AuNPs were displayed with three different diameters

under TEM, 58 nm, 76 nm, 100 nm, respectively (Figure 2A and Figure 3), when the amount of spherical AuNPs decreased from 600 μ L, 300 μ L to 100 μ L, while HAuCl₄, hydroquinone, sodium citrate amounts kept fixed. It turned out that the bigger SUL-AuNPs size, the more nanothorns synthesized on spherical Au surface. Hence, 100 nm SUL-AuNPs displayed better preferable sea urchin morphologies and calculated concentrations of synthesized SUL-AuNPs are 54 μ g/mL (Figure 2A, e&f). Consequently, to obtain better morphologies of SUL-AuNPs, a lower concentration of

AuNPs seeds was favored in the reaction system. The color of the synthesized SUL-AuNPs solution displayed turned to green-pink from pink (Figure 2B), implying the morphology variation of SUL-AuNPs. Meanwhile, the UV-vis absorption of SUL-AuNPs shifted from 550 nm to 650 nm (Figure 2C), as a result of an increase of SUL-AuNPs diameters, which was consistent with their optical observation (Figure 2B), while the spherical AuNPs with a diameter of 20 nm have an absorption at 520 nm (Figure 4). The calculated concentrations of synthesized SUL-AuNPs are 54 μ g/mL.

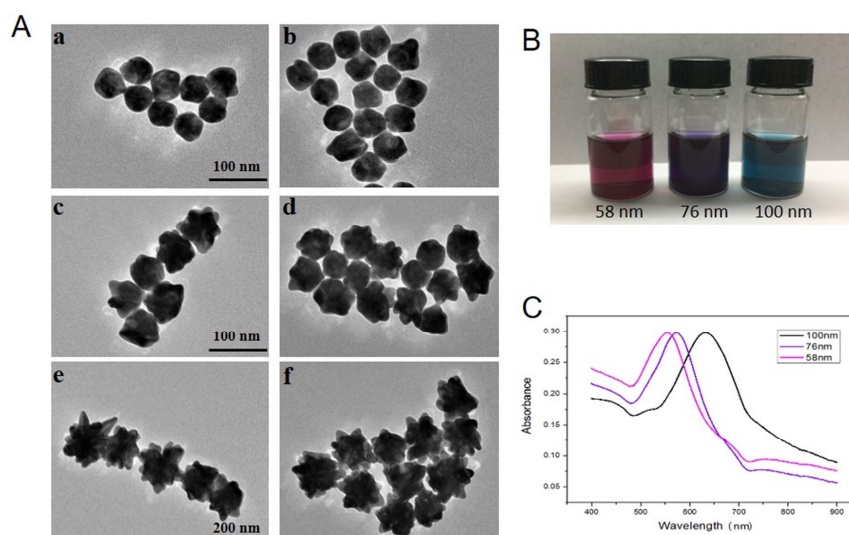
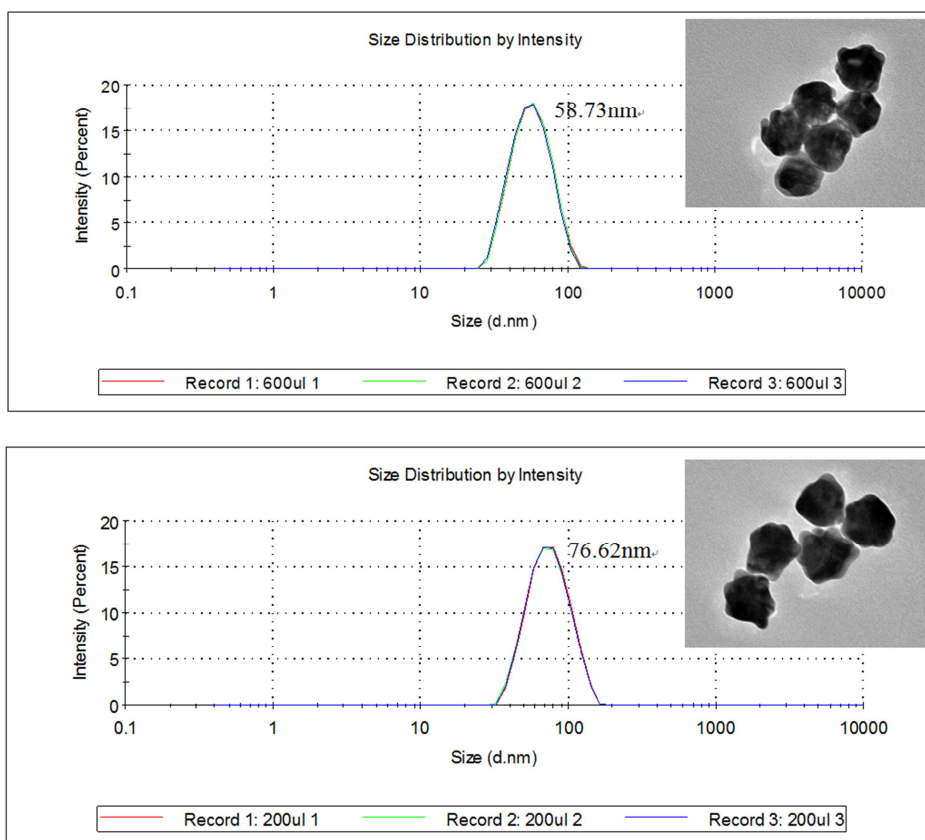


Figure 2. (A) Influence of the AuNPs seeds amounts on the morphologies of SUL-AuNPs, 100 μ L (a) (b), 300 μ L (c) (d), 600 μ L (e) (f). (B) Influence of the AuNPs seeds amounts on the optical observation of synthesized SUL-AuNPs. (C) UV-vis absorption spectra of the as-prepared SUL-AuNPs.



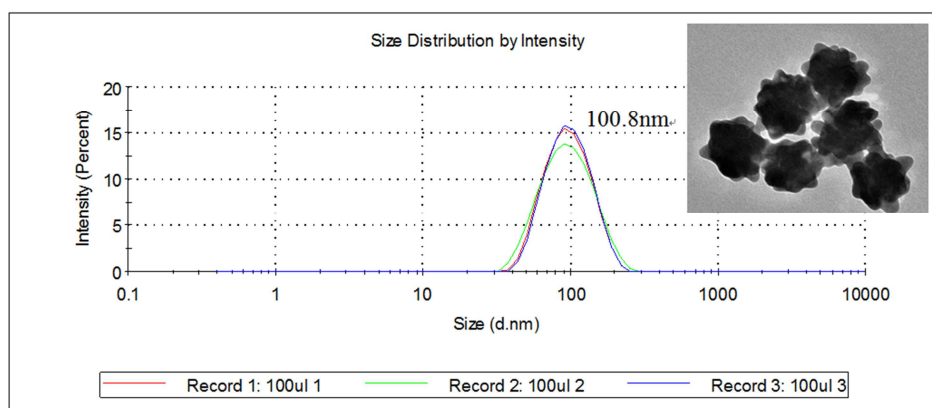


Figure 3. Characterization of size distribution of synthesized SUL-AuNPs.

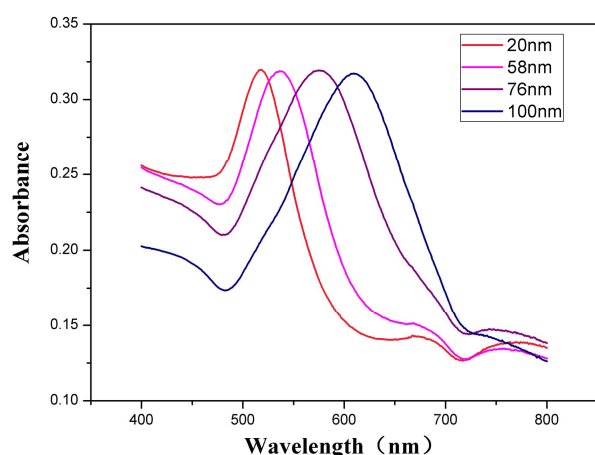


Figure 4. UV-vis absorption spectra of 20 nm Au seeds and the as-prepared SUL-AuNPs.

To obtain the optimal GSH detection condition, 100 nm SUL-AuNPs with preferable morphologies was used for RB-SUL-AuNPs synthesis. Figure 5 showed that the fluorescence intensity of RB enhanced dramatically when increase added GSH concentrations, indicating that RB were released from SUL-AuNPs because of GSH competitive binding. The effect of the reaction time for GSH detection was also investigated. After the addition of GSH for 60 mins, the fluorescence intensity of RB became constant and keep stable for at least 1hr. Hence, we selected 60 mins as the optimized reaction time for GSH detection using 100 nm SUL-AuNPs.

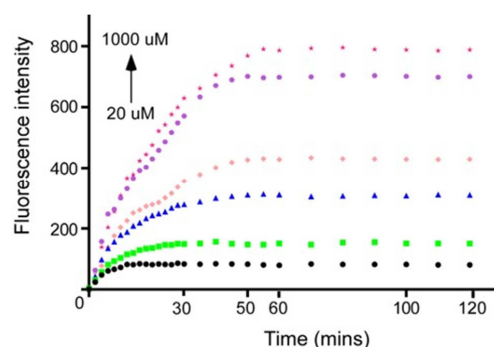


Figure 5. Influence of GSH concentration and reaction time on the fluorescence intensity of RB-SUL-AuNPs. GSH concentration increased from 20 μ M, 50 μ M, 100 μ M, 200 μ M, 500 μ M, to 1000 μ M, respectively. Fluorescence intensity was measured at 578 nm.

We further tested the fluorescence intensity of released RB from RB-SUL-AuNPs by adding different GSH concentrations under the optimized reaction conditions. As shown in Figure 6A, the fluorescence intensity of RB was increased with increased GSH concentrations at 578 nm. Figure 6B displayed the relationships ($R^2=0.9888$) between the fluorescence intensity and the concentration of added GSH. The inset of Figure 6B showed a linear relationship between the fluorescence intensity and the added GSH concentrations from 2 μ M to 100 μ M. Effect of GSH concentrations on the fluorescent intensity of 58 nm and 76 nm RB-SUL-AuNPs were also investigated (Figure 7), which showed lower GSH detection sensitivity compared with 100 nm SUL-AuNPs.

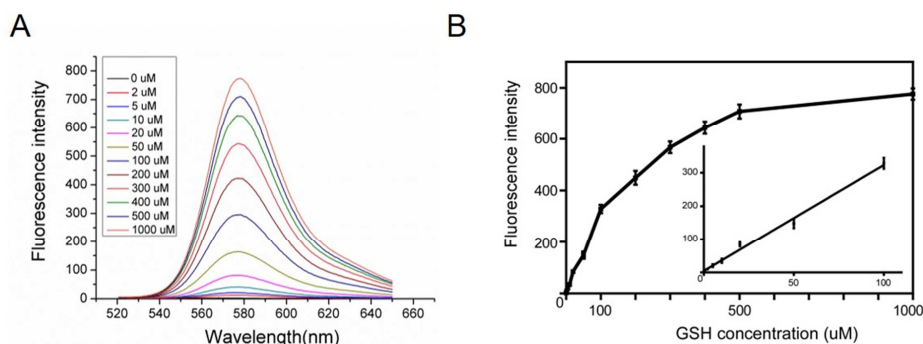


Figure 6. Effect of GSH concentration on the fluorescence intensity of RB-SUL-AuNPs. (A) GSH concentration increased from 2 μ M to 1000 μ M. Fluorescence intensity was measured at 578 nm with 100 nm SUL-AuNPs. (B) The calibration curve of fluorescent intensity at different GSH concentrations was provided.

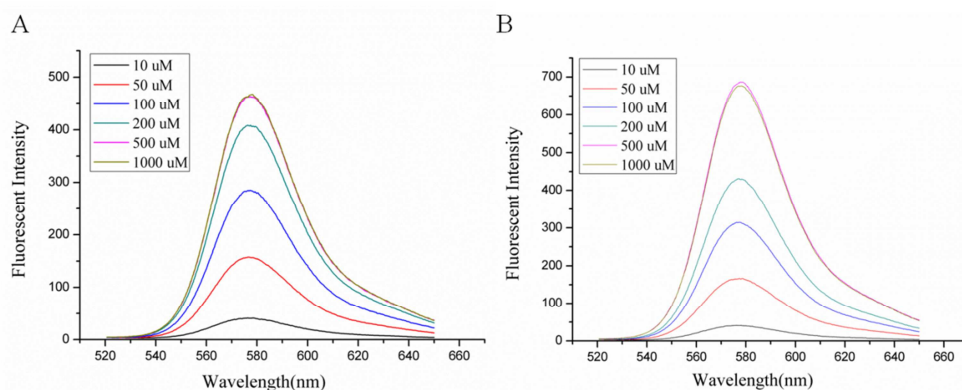


Figure 7. Effect of GSH concentrations on the fluorescent intensity of RB-SUL-AuNPs. GSH concentration increased from 10 μM to 1000 μM . Fluorescent intensities were measured at 578 nm with different SUL-AuNPs, 58 nm (A), 76 nm (B).

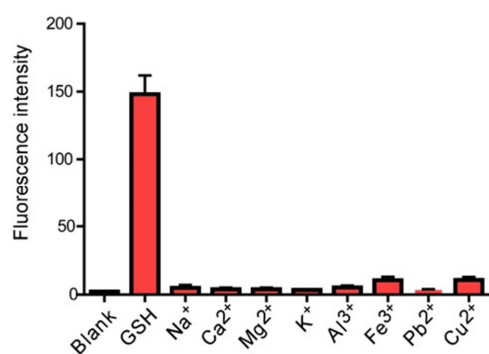


Figure 8. The fluorescence intensity of RB-SUL-AuNPs in the presence of different metal ions. The concentration of GSH and the concentration of metal ions are 50 μM . RB-SUL-AuNPs only solution was used as Blank.

The influences resulted from coexisting ions in the reaction solution were simply tested since the interference came from amino acids, proteins and other thiol species is negligible in hepatocytes. To test the selectivity of RB-SUL-AuNPs (100 nm SUL-AuNPs) for GSH in hepatocytes, several metal ions, including Na^+ , Ca^{2+} , Mg^{2+} , K^+ , Al^{3+} , Fe^{3+} , Pb^{2+} and Cu^{2+} , were tested at the concentrations of 50 μM . As shown in Figure 8, none obvious fluorescence changes of RB-SUL-AuNPs was observed under the same GSH reaction condition, indicating that the tested metal ions have little influence on hepatocytes

cellular thiols detection using RB-SUL-AuNPs.

To test cellular use of SUL-AuNPs for GSH detection, flow cytometry assay was applied to characterize the HepG2 cells fluorescence signals in the presence of RB-SUL-AuNPs (Figure 9A). When HepG2 cells were incubated with RB-SUL-AuNPs (2 nm) for 24 hrs, intracellular fluorescence dramatically increased compared with 20 nm Au seeds, and the bigger diameter size, the higher fluorescence increase. 100 nm SUL-AuNPs displayed highest fluorescence intensity increase compared to the other two sizes of SUL-AuNPs at the same reaction condition. Normal hepatocytes L02 cells were also applied at the same reaction condition and the results displayed lower fluorescence intensity compared with HepG2 cells (Figure 9B), which was consistent with previous study that hepatoma HepG2 cells contain high levels of GSH [29]. Meanwhile, this result also indicates that our synthesized SUL-AuNPs are membrane-permeable. Furthermore, the intercellular GSH detection using RB-SUL-AuNPs in hepatoma HepG2 cells extracts can also be observed through naked eye. Incubated HepG2 cells extracts with RB-SUL-AuNPs (100 nm SUL-AuNPs) for 1 hr, the HepG2 cells lysate supernatant showed a bright pink (Figure 10). Conclusively, it seems that SUL-AuNPs provides a quick qualitative estimating of cellular thiols instead of quantitative estimation.

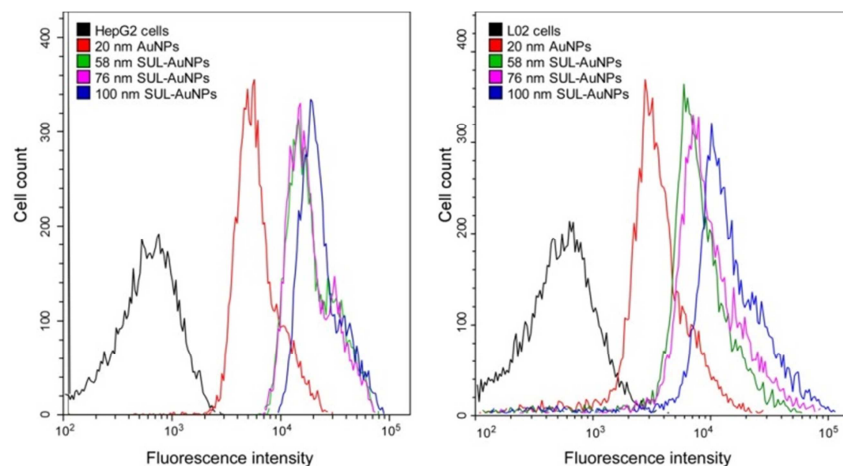


Figure 9. Flow cytometry assay of fluorescent signals in HepG2 cells (A) and L02 cells (B) before and after incubation with RB-SUL-AuNPs.

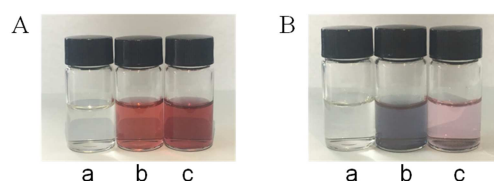


Figure 10. Visual detection of thiols in HepG2 cell extracts using (A) 20 nm Au seeds, (B) 100 nm SUL-AuNPs. (a) HepG2 cell extracts, (b) RB & Au NPs only, (c) HepG2 cell extracts in the presence of RB & Au NPs, respectively.

The cytotoxicity of the SUL-AuNPs in HepG2 cells and L02 cells were furtherly studied by CCK-8 assay. As the data shown in Figure 11, it could be concluded that the SUL-AuNPs have no cytotoxicity to either HepG2 cells or L02 cells under the indicated concentrations.

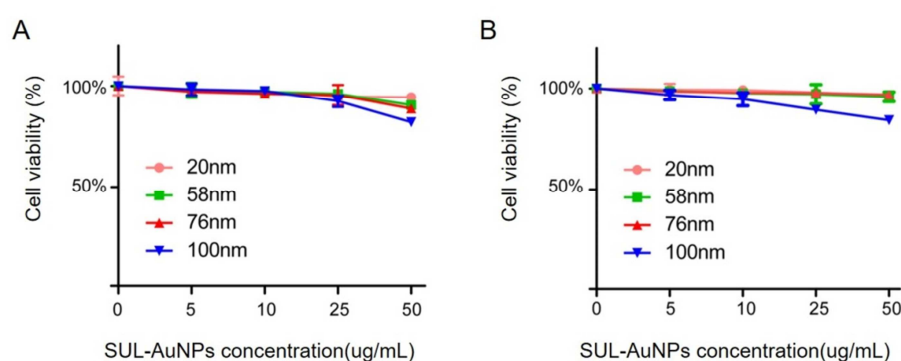


Figure 11. Relative cell viabilities of HepG2 cells (A) and L02 cells (B) after incubation with 20 nm AuNPs and SUL-AuNPs, 58 nm, 76 nm, 100 nm, respectively.

4. Conclusions

In summary, we synthesized three different diameters of SUL-AuNPs based on spherical AuNPs seed-mediated growth method by altering the amount of AuNPs in reaction system. SUL-AuNPs sizes vary from 58 nm to 100 nm and extinction spectrum shows a shift from 550 nm to 650 nm. RB functionalized SUL-AuNPs was successfully applied for GSH detection in hepatocytes and cell extracts, among them, 100 nm SUL-AuNPs showed preferable morphologies and highest sensitivity. RB-SUL-AuNPs coupled with FRET for GSH detection, which we developed, provided many advantages, such as simplicity of preparation and without specific instruments. What's more, the synthesized SUL-AuNPs turned out membrane-permeable, and displayed ignorable cytotoxicity, which make SUL-AuNPs promising cellular thiols detection probes in nanodiagnosis.

Author Contributions

Ting Lei Zhao and Zhe Zhang carried out most of the experimental work; Dan Li participated in data collection and analysis; Yanxialei Jiang conceived of the study, coordinated the research and helped draft the manuscript. All authors gave final approval for publication and agree to be held accountable for the work performed therein.

Conflicts of Interest

There are no conflicts to declare.

Ethics

This article does not present research with ethical considerations.

Funding

This work was supported by the China Scholarship Council (202108370145).

References

- [1] Wilson, R., *The use of gold nanoparticles in diagnostics and detection*. Chemical Society Reviews, 2008. 37 (9): p. 2028-2045.
- [2] Mirkin, C. A., et al., *A DNA-based method for rationally assembling nanoparticles into macroscopic materials*. Nature, 1996. 382 (6592): p. 607-609.
- [3] Wei, X., et al., *A colorimetric sensor for determination of cysteine by carboxymethyl cellulose-functionalized gold nanoparticles*. Anal Chim Acta, 2010. 671 (1-2): p. 80-84.
- [4] Qian, R., Y. Cao, and Y. T. Long, *Dual-Targeting Nanovesicles for In Situ Intracellular Imaging of and Discrimination between Wild-type and Mutant p53*. Angew Chem Int Ed Engl, 2016. 55 (2): p. 719-723.
- [5] Yuan, H., et al., *Gold nanostars: surfactant-free synthesis, 3D modelling, and two-photon photoluminescence imaging*. Nanotechnology, 2012. 23 (7): p. 075102.

- [6] Wang, X., et al., *Hierarchically assembled Au microspheres and sea urchin-like architectures: formation mechanism and SERS study*. *Nanoscale*, 2012. 4 (24): p. 7766-7772.
- [7] Li, J., et al., *Controllable synthesis and SERS characteristics of hollow sea-urchin gold nanoparticles*. *Physical Chemistry Chemical Physics Pccp*, 2014. 16 (46): p. 25601-25608.
- [8] Wang, L., et al., *Sea-urchin like Au nanoclusters with surface enhanced Raman scattering in detecting EGFR mutation status of malignant pleural effusion*. *Acs Appl Mater Interfaces*, 2015. 7 (1): p. 359-369.
- [9] Jun-Peng, L. I., et al., *SERS Characteristics of Sea Urchin-like Gold Nanoparticles Dependent on Their Surface Morphology*. *Acta Photonica Sinica*, 2015. 44 (4): p. 13-17.
- [10] Chen, X., et al., *Fluorescent and colorimetric probes for detection of thiols*. *Cheminform*, 2010. 39 (6): p. 2120-2135.
- [11] Sreejith, S., K. P. Divya, and A. Ajayaghosh, *A near-infrared squaraine dye as a latent ratiometric fluorophore for the detection of aminothiol content in blood plasma*. *Angewandte Chemie*, 2010. 47 (41): p. 7883-7887.
- [12] Chang, S. L., et al., *Ratiometric Detection of Mitochondrial Thiols with a Two-Photon Fluorescent Probe*. *Journal of the American Chemical Society*, 2011. 133 (29): p. 11132-11135.
- [13] Roslis, J. V., et al., *Squaraines as fluoro-chromogenic probes for thiol-containing compounds and their application to the detection of biorelevant thiols*. *Journal of the American Chemical Society*, 2004. 126 (13): p. 4064-4065.
- [14] Hwang, C., A. J. Sinskey, and H. F. Lodish, *Oxidized redox state of glutathione in the endoplasmic reticulum*. *Science*, 1992. 257 (5076): p. 1496-1502.
- [15] Hong, R., et al., *Glutathione-mediated delivery and release using monolayer protected nanoparticle carriers*. *J Am Chem Soc*, 2006. 128 (4): p. 1078-1079.
- [16] Rybka, J., et al., *Glutathione-Related Antioxidant Defense System in Elderly Patients Treated for Hypertension*. *Cardiovascular Toxicology*, 2011. 11 (1): p. 1-9.
- [17] Lapenna, D., et al., *Glutathione-Related Antioxidant Defenses in Human Atherosclerotic Plaques*. *Circulation*, 1998. 97 (19): p. 1930-1934.
- [18] Cnubben, N. H., et al., *The interplay of glutathione-related processes in antioxidant defense*. *Environmental Toxicology & Pharmacology*, 2001. 10 (4): p. 141-152.
- [19] Zhao, M., et al., *GSH-dependent antioxidant defense contributes to the acclimation of colon cancer cells to acidic microenvironment*. *Cell Cycle*, 2016. 15 (8): p. 1125-1133.
- [20] Kim, J. S. and D. T. Quang, *Calixarene-derived fluorescent probes*. *Chem Rev*, 2007. 107 (9): p. 3780-3799.
- [21] Hohng, S., et al., *Maximizing information content of single-molecule FRET experiments: multi-color FRET and FRET combined with force or torque*. *Chem Soc Rev*, 2014. 43 (4): p. 1007-1013.
- [22] Berney, C. and G. Danuser, *FRET or No FRET: A Quantitative Comparison*. *Biophysical Journal*, 2003. 84 (6): p. 3992-4010.
- [23] Oh, E., et al., *Inhibition assay of biomolecules based on fluorescence resonance energy transfer (FRET) between quantum dots and gold nanoparticles*. *Journal of the American Chemical Society*, 2005. 127 (10): p. 3270-3271.
- [24] Cai, H. H., et al., *Naked eye detection of glutathione in living cells using rhodamine B-functionalized gold nanoparticles coupled with FRET*. *Dyes & Pigments*, 2016. 92 (1): p. 778-782.
- [25] Wei, S., et al., *A novel self-quenching system based on bis-naphthalimide: a dual two-photon-channel GSH fluorescent probe*. *Chem Asian J*, 2017. 12 (13).
- [26] Ahmad, M., et al., *Real-time monitoring of glutathione in living cells using genetically encoded FRET-based ratiometric nanosensor*. *Scientific Reports*, 2020. 10 (1): p. 992.
- [27] Zhang, H. and D. Wang, *Controlling the growth of charged-nanoparticle chains through interparticle electrostatic repulsion*. *Angew Chem Int Ed Engl*, 2008. 47 (21): p. 3984-3987.
- [28] Li, J., et al., *Controllable Synthesis of Stable Urchin-like Gold Nanoparticles Using Hydroquinone to Tune the Reactivity of Gold Chloride*. *The Journal of Physical Chemistry C*, 2011. 115 (9): p. 3630-3637.
- [29] Jiang, Y., et al., *An ultrasensitive fluorogenic probe for revealing the role of glutathione in chemotherapy resistance*. *Chem Sci*, 2017. 8 (12): p. 8012-8018.